

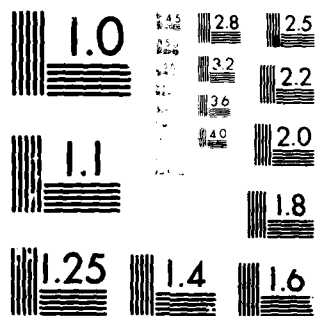
CASE WESTERN RESERVE UNIV CLEVELAND OHIO DEPT OF MACR--ETC F/G 11/9  
DEVELOPMENT OF HARD ELASTIC SOLIDS FROM GLASSY POLYMERS.(U)  
JUN 80 A MOET, I PALLEY, E BAER N00014-75-C-0795

TR-10

NL

$$\frac{\Delta E}{E} = \frac{\Delta \lambda}{\lambda} = \frac{\Delta \lambda}{\lambda_0 + \lambda_D}$$

END  
DATE  
FILMED  
7-80  
DTIC



MICROCOPY RESOLUTION TEST CHART  
NATIONAL BUREAU OF STANDARDS-1963-A

ADA 085804

800 619 08

SECURITY CLASSIFICATION OF THIS PAGE (When Data Entered)

REPORT DOCUMENTATION PAGE		READ INSTRUCTIONS BEFORE COMPLETING FORM
1. REPORT NUMBER Technical Report 10	2. GOVT ACCESSION NO. AD-A085-804	3. RECIPIENT'S CATALOG NUMBER 9. Colvin. 4. rpt.
4. TITLE (and Subtitle) DEVELOPMENT OF HARD ELASTIC SOLIDS FROM GLASSY POLYMERS.	5. TYPE OF REPORT & PERIOD COVERED Technical Report Interim	
7. AUTHOR(s) Abdelsamie Moet, Igor Palley Eric Baer	6. PERFORMING ORG. REPORT NUMBER	
9. PERFORMING ORGANIZATION NAME AND ADDRESS Department of Macromolecular Science Case Western Reserve University Cleveland, Ohio 44106	8. CONTRACT OR GRANT NUMBER(s) N00014-75-0795	
11. CONTROLLING OFFICE NAME AND ADDRESS Office of Naval Research (Code 472) Arlington, Virginia 22217	10. PROGRAM ELEMENT, PROJECT, TASK AREA & WORK UNIT NUMBERS	
14. MONITORING AGENCY NAME & ADDRESS (if different from Controlling Office) 1256	12. REPORT DATE June 1980	
	13. NUMBER OF PAGES	
	15. SECURITY CLASS. (of this report) Unclassified	
	16a. DECLASSIFICATION/DOWNGRADING SCHEDULE	
16. DISTRIBUTION STATEMENT (of this Report) Approved for public release; distribution unlimited. Reproduction in whole or in part is permitted for any purpose of the United States Government.		
17. DISTRIBUTION STATEMENT (of the abstract entered in Block 20, if different from Report)		
18. SUPPLEMENTARY NOTES A		
19. KEY WORDS (Continue on reverse side if necessary and identify by block number) Hard Elastic, Fiber, Film, Fibrillar, Craze, Lamellae Elastic Recovery, Thermoelastic, Healing, Work Recovery, Cyclic Loading, Viscoelastic, Conformational, Energetic, Stress Relaxation, Environmental Liquids, Free Surface, Surface Force, Surface Tension, Sequential Fibrillation.		
20. ABSTRACT (Continue on reverse side if necessary and identify by block number) High impact polystyrene (HIPS) has been processed into a specific microstructure which exhibited the hard elastic behavior previously restricted to crystalline polymers. Unidirectionally stacked profuse crazes formed in uniaxially elongated HIPS reproduced morphologies resembling the row nucleated structures of stacked lamellar aggregates bridged by extended fibrils. Films in this form possess repeated high recovery from large extension without rupture. Stress-strain and stress-relaxation tests		

DD FORM 1 JAN 73 1473

EDITION OF 1 NOV 65 IS OBSOLETE  
S/N 0102-014-6601

SECURITY CLASSIFICATION OF THIS PAGE (When Data Entered)

408357

4/3

DDC FILE COPY

performed in air and in a variety of liquids in addition to thermoelastic experiments indicate that this novel material has identical characteristics to that of hard elastic crystalline polymers. The time-independent component of elastic recovery was found to be an energy driven process which originates largely from surface forces. Our results confirm that the recovery process of elastic HIPS, like crystalline systems, is composed of an instantaneous component in addition to time-dependent healing mechanism. The first was found to be energetic in nature whereas the second remained conformational (entropic). A structural model is presented which explains the observed mechanical and structural data. The model is based on the reversible extensive formation of fresh surface of the craze (or interlamellar) fibrillar material giving rise to the elastic restorative force. Time-dependent "healing" stems from the conformational character maintained by the subfibrils. Stress-induced sorption and release of liquid, a newly discovered property, is also discussed.

Accession Number	
1	
2	
3	
4	
5	
6	
7	
8	
9	
10	
11	
12	
13	
14	
15	
16	
17	
18	
19	
20	
21	
22	
23	
24	
25	
26	
27	
28	
29	
30	
31	
32	
33	
34	
35	
36	
37	
38	
39	
40	
41	
42	
43	
44	
45	
46	
47	
48	
49	
50	
51	
52	
53	
54	
55	
56	
57	
58	
59	
60	
61	
62	
63	
64	
65	
66	
67	
68	
69	
70	
71	
72	
73	
74	
75	
76	
77	
78	
79	
80	
81	
82	
83	
84	
85	
86	
87	
88	
89	
90	
91	
92	
93	
94	
95	
96	
97	
98	
99	
100	

CASE WESTERN RESERVE UNIVERSITY  
Department of Macromolecular Science  
Cleveland, Ohio 44106

Technical Report No. 10

DEVELOPMENT OF HARD ELASTIC SOLIDS FROM GLASSY POLYMERS

BY

Abdelsamie Moet, Igor Palley and Eric Baer  
Department of Macromolecular Science  
Case Western Reserve University  
Cleveland, Ohio 44106

May 19, 1980

Research Sponsored by the  
Office of Naval Research

Contract N00014-75-C-0795

### ABSTRACT

High impact polystyrene (HIPS) has been processed into a specific microstructure which exhibited the hard elastic behavior previously restricted to crystalline polymers. Unidirectionally stacked profuse crazes formed in uniaxially elongated HIPS reproduced morphologies resembling the row nucleated structures of stacked lamellar aggregates bridged by extended fibrils. Films in this form possess repeated high recovery from large extension without rupture. Stress-strain and stress-relaxation tests performed in air and in a variety of liquids in addition to thermoelastic experiments indicate that this novel material has identical characteristics to that of hard elastic crystalline polymers. The time-independent component of elastic recovery was found to be an energy driven process which originates largely from surface forces.

Our results confirm that the recovery process of elastic HIPS, like crystalline systems, is composed of an instantaneous component in addition to time-dependent healing mechanism. The first was found to be energetic in nature whereas the second remained conformational (entropic). A structural model is presented which explains the observed mechanical and structural data. The model is based on the reversible extensive formation of fresh surface of the craze (or interlamellar) fibrillar material giving rise to the elastic restorative force. Time-dependent "healing" stems from the conformational

character maintained by the subfibrils. Stress-induced sorption and release of liquid, a newly discovered property, is also discussed.

## I. INTRODUCTION

Recently we reported on the development of hard elastic material from high impact polystyrene (HIPS), an amorphous glassy polymer, by the induction of profuse crazing stacked perpendicular to the applied uniaxial tension.<sup>1</sup> Until then, hard elastic behavior was thought to be acquired only from crystalline polymers<sup>2</sup> by a combination of melt extrusion and stress crystallization followed by annealing under tensile stress. This treatment produced a structure composed of fibril-bridged lamellar aggregates stacked perpendicular to the applied stress.<sup>3, 4</sup> The interlamellar fibril-bridged gaps observed in hard elastic crystalline polymers are similar to craze fibrils occurring in glassy polymers. Thus, it was predicted that both structures, irrespective of crystallinity, should produce the same property hard elasticity. The stress-strain curve of profusely crazed polycarbonate (PC) during loading and unloading, recently reported by Shultz and coworkers,<sup>5</sup> reflects definite hard elastic character. This behavior was caused by profuse crazing developed during cyclic deformation. It is obvious, therefore, that glassy polymers, whether two phase (e. g., HIPS) or one phase (e. g., PC), can be processed by judicious crazing into hard elastic material. An essential requirement, however, appears to be the introduction of a large density of minute crazes in order to induce a morphology close enough to that of crystalline hard elastic materials.



The development of models to expound hard elastic behavior has been based upon the knowledge available at the time of such development. Due to the fact that hard elastic behavior had been observed only in row crystallized polymers, the majority of the present models attributed the restoring force causing elastic recovery from large deformations to some mechanism within the crystalline lamellae. A common feature of such models is the postulation of some sort of interlamellar tie molecules. As a result of having interlamellar tie "points", the structural models operate through lamellar shear (paper bell model),<sup>6</sup> leaf spring and unspecified tie point elasticity,<sup>7</sup> reversible fracture and bending of lamellae,<sup>8</sup> paracrystalline effects,<sup>9</sup> or by increasing of the intermolecular distances within the lamellae against van der Waal's force.<sup>10</sup> Microscopic evidence, however, clearly shows no sign of lamellar shear or bending.<sup>3,4</sup> Instead, the lamellae are found to undergo lateral translation in a parallel fashion with the bridging fibrils always in an extended state. This, in addition to the discovery of hard elastic glassy polymer behavior, obviously suggests that a physical mechanism of hard elastic behavior cannot be based on lamellar deformations. Extended fibrils bridging solid entities is the common feature in both crystalline and glassy materials. Few authors, however, have recognized that the fibrils bridging

interlamellar gaps are to some extent responsible for the elasticity of these materials via surface forces<sup>1, 3, 11</sup> or orientation effects.<sup>12</sup>

This paper, a part of a more extensive program to establish processing techniques and characterize hard elastic glassy polymers, reports results of stress-strain measurements, relaxation studies in air and in liquids of varying activities, and also thermoelastic behavior. In addition, new developments to amplify and support the model suggested earlier<sup>1</sup> are also summarized.

## II. EXPERIMENTAL

The material used in our investigation was ordinary high impact polystyrene (HIPS) generously supplied by the Dow Chemical Company. Dumbbell-shaped specimens about 3mm wide and 16mm gauge length were cut from compression molded sheets about 0.25mm thick. The specimens were subsequently annealed in a vacuum oven at 86 °C for 50 hours, slowly cooled at 10 °C/hour to room temperature and stored in a desiccator. Hard elastic material was obtained by straining the specimen in an Instron at  $3 \times 10^{-2} \text{ min}^{-1}$  to a known elongation (referred to as crazing elongation) after which the specimen was unloaded and allowed to hang load-free for a period of 10 minutes, unless otherwise stated. Subsequently, a strain rate of  $1.3 \times 10^{-2} \text{ min}^{-1}$  was used to test these samples for hard elastic behavior during loading and unloading.

Four basic types of tests were performed: stress-strain (referred to as hard elastic cycle), stress-relaxation in air and in various liquids, thermoelastic measurements, and stress-controlled imbibing and release of high viscosity silicone oil. Tests requiring temperature control were conducted in a forced air heated oven in which the temperature was kept within  $\pm 1$  °C. Imbibing and release experiments were conducted in a stress-relaxation mode as explained in the next section.

### III. RESULTS AND DISCUSSION

As shown in Fig. 1 and subsequent figures, the stress-strain curve during loading (extension) and unloading (recovery), i. e. , hard elastic cycle, clearly follows four different stages. In stage I, the material exhibits Hookian behavior followed by a yield "point". A complex stress-strain behavior is identified as stage II which may or may not be followed by a stress plateau identified as stage III. Finally, stage IV identifies the recovery process occurring during unloading.

#### A. Factors affecting the mechanical behavior

##### 1. Precrazing intensity

Hard elastic behavior of glassy polymers is generally induced by profuse crazing. In order to study the effect of precrazing intensity on the hard elastic behavior of HIPS, samples were stretched to various crazing elongations at a constant strain rate after which they were unloaded for 10 minutes. Subsequently, these samples were tested for stress-strain behavior. Typical stress-strain curves of samples precrazed to 30%, 50% and 70% elongations are shown in Fig. 1. All three reveal conventional hard elastic behavior. Thickness measurements during elongation showed no significant decrease in cross-sectional area. The samples precrazed to more than 60% elongation did not exhibit a stress plateau up to a hard elastic strain of 0.4 (stage III). Instead, a higher plateau would

have occurred at a strain of 0.5 or more. Upon load reversal, the stress decreased to zero and most of the strain was recovered (stage IV). While high recovery from such large elongation is an important aspect, the mechanical behavior exhibited other unique features, some of which are discussed below.

The initial value of Young's modulus, estimated for 30% precrazed material, was found to be  $3 \times 10^3 \text{ kg/cm}^2$  which is an order of magnitude lower than that of ordinary HIPS. Taking into account the geometrical model of precrazed HIPS reported earlier,<sup>1</sup> it becomes clear that the low modulus reflects the composite nature of the system. If the system is presumably reduced into two phases: craze fibrils and HIPS blocks assembled in series,<sup>13</sup> one obtains an average initial Young's modulus for craze material of about  $1.3 \times 10^3 \text{ kg/cm}^2$ . This value is based on a craze volume fraction of 0.3, roughly estimated from an electron micrograph of crazed thin film cast from the same batch. It is also noticeable that the initial modulus value decreased as the precrazing strain increased. If the series model for modulus calculation holds, then the volume fraction of crazed material may have increased with higher precrazing strain. This increase may be a result of craze widening since the craze length is constrained by two rubber particles and the number of crazes at these levels of precrazing strain is almost unchanged. The idea of higher fractional volume of craze material at higher

precrazing strain may also explain the reduction in initial yield stress, the lowering of stress during stage II, and the elevation of stage III plateau stress.

Although the extension path was dependent on precrazing conditions, the recovery path (stage IV) was totally independent. Furthermore, the initial modulus of recovery estimated from Fig. 1 was found to be  $6.3 \times 10^4 \text{ kg/cm}^2$ , an order of magnitude higher than the average initial Young's modulus. Perhaps this observation is indicative of the magnitude of orientation that the craze material undergoes in the course of elongation. Noticeably, the elastic recovery of hard elastic HIPS estimated at 75% is comparable to that of crystalline hard elastic material such as poly-3-methylbutene-1<sup>14</sup> and slightly lower than others such as polypropylene.<sup>7</sup>

## 2. Effects of repeated cyclic loading

Continuous and intermittent cyclic experiments were conducted to determine the effect of repeated loading on the hard elastic behavior of precrazed HIPS. The stress-strain curves for 12 continuous cycles to 40% extension are shown in Fig. 2a. The initial modulus and the yield "point" were lowered, and the elastic and work recovery were considerably decreased within the first few cycles; eventually these approached constant values in subsequent cycles. After several repeated cycles (approximately 8), the extension and recovery paths

became practically unchanged. Notice that the change in the recovery paths over the first few cycles are much smaller than those in the corresponding extension paths. This behavior is identical to that of hard elastic polypropylene (PP) as reported by Park and Noether.<sup>15</sup>

The stress-strain behavior for three intermittent cycles to 40% extension is shown in Fig. 2b. Contrary to the continuous case, subsequent loading after one hour resulted in a substantial increase in the initial yield stress and a smaller increase in Young's modulus. In addition, the plateau (stage III) was shifted from about 0.30 to 0.38 strain. In the third cycle (after one day), similar changes were observed except that the plateau in this cycle was not observed up to 40% extension. The retraction path, again, was independent of the extension history. In addition, the elastic recoverability remained almost unchanged. These observations bear striking resemblance to results reported earlier on semicrystalline hard elastic polymers.<sup>2, 4, 7</sup>

The contrasting results of continuous and intermittent loading reflect the complex nature of the phenomenon, however, two recovery processes may be inferred: an instantaneous elastic recovery process accompanied by a time-dependent "healing" mechanism.

### 3. Effects of elapsed time

In another experiment, the effects of time elapsed between precrazing and testing for hard elastic behavior, i. e., shelf life,

were considered. Results of this experiment are displayed in Fig. 3. The rise observed in the yield stress at 100 minutes is reminiscent of the healing mechanism which is known to occur in such profusely crazed systems.<sup>16</sup> This healing may also be inferred from the lowering of the plateau stress with increased shelf life. The retractive stress-strain behavior and the elastic recovery, however, showed little or no dependence on the elapsed time up to 100 minutes.

#### 4. Effect of temperature

Figure 4 exhibits hard elastic cycles of identical samples, precrazed at room temperature and tested at 42°, 62°, and 85 °C. As expected, the initial Young's modulus decreased with temperature. Note, however, that a more defined yield point accompanied by yield instability occurred at 42 °C and persisted at higher temperatures. The development of this yield behavior provides more evidence supportive for the idea of healing in the fibrillar structure of the craze. The elastic recovery also diminished as the test temperature was raised. It is important, however, that even at 85 °C, which is about 10 °C below the glass transition, the material still showed elastic recovery of about 50%. In addition, a well defined plateau (stage III) appeared at 85 °C although its level approached that of constant stress deformation.

The above results indicate clearly that the stress-strain curves of precrazed HIPS exhibit hard elastic character identical to



that displayed by crystalline hard elastic polymers. Similar stress-strain behavior has been reported from a single craze of polycarbonate,<sup>17</sup> and polystyrene.<sup>18</sup> Taking into account that a craze is but fibrillated material extended between solid boundaries, it is therefore obvious that the well recognized phenomenon of hard elasticity is a manifestation of the fibrillar structure bridging the layers of solid material whose surface is oriented normal to the applied tensile stress. Since solid lamellar islands do not exist in the precrazed amorphous material, restricting the phenomenon to crystalline polymeric systems<sup>2</sup> or explaining the mechanism on the basis of lamellar bending, shear, or adhesive fracture<sup>4, 6-10</sup> is structurally unsound.

The fact that some systems exhibit higher elastic recovery than others remains to be investigated. However, comparison of the stress-strain behavior of precrazed PC<sup>5</sup> with that of a single PC craze<sup>17</sup> reveals the dramatic increase in the elastic recovery of the former over the latter. Similar conclusions may be reached by comparing our stress-strain results (Figs. 1-3) with the cyclic stress-strain curves of HIPS reported earlier by Bucknall.<sup>19</sup> Thus, the alternation of fibrillar domains with solid islands, in a multiple fashion may be essential for high recovery from large strains. The volume fraction of the fibrillar elements (inclusions) in the sample appears to be another important factor.

B. Thermoelastic behavior

In order to determine the nature of the elastic forces responsible for hard elasticity in our system, the retractive force was measured as a function of temperature at a constant elongation of 25%. Results of these measurements are presented in Fig. 5. The sample was allowed to relax from the fixed elongation at 62 °C until the rate of stress decay had become small compared to the time scale of the experiment. While the system was cooled down, the load was recorded at selected temperature intervals. The sample was then equilibrated at room temperature for several minutes before starting the next half cycle (heating) to check reversibility.

Basic thermodynamic considerations dictate that the retractive force in elastic deformation must equal the sum of the entropy and the internal energy effects. This rule provides a direct means to determine experimentally the entropic as well as the energetic changes due to deformation, given that the process is reversible. The reversible relationship describing the thermoelastic behavior of hard elastic HIPS (Fig. 5), as in other hard elastic materials,<sup>12, 14</sup> exhibits a negative slope which is contrary to the known rubber-like behavior. It is thus suggestive that hard elasticity must be controlled by an energy dominated mechanism. Of course, this

prediction is purely phenomenological and does not imply any particular mechanism. It is in the interpretation of these results, taking other experimental and morphological observations into account, that a physical model may be developed (see Section IV).

A noticeable difference between the thermoelastic behavior of precrazed HIPS and that of Celcon, a crystalline system, lies in the temperature coefficient of the elastic force. An estimated coefficient of about  $1.6 \times 10^6 \text{ dynes/cm}^2 \text{ } ^\circ\text{C}$  for Celcon<sup>14</sup> is an order of magnitude higher than that of HIPS which is about  $1.3 \times 10^5 \text{ dynes/cm}^2 \text{ } ^\circ\text{C}$ . On the other hand, polybutene-1,<sup>12</sup> another crystalline hard elastomer film, showed a coefficient of about  $2 \times 10^4 \text{ dynes/cm}^2 \text{ } ^\circ\text{C}$ , which is an order of magnitude lower than that of HIPS elastomer. Although the established negative slope of the force-temperature relationship indicates a dominant energetic contribution for all three polymers, its magnitude may be considered as a means to evaluate that contribution. The difference observed in thermoelastic coefficient may denote competition between energetic and entropic contributions<sup>2, 11</sup> due to a combination of molecular and structural parameters; the latter is strongly dependent on the processing and deformation history.

#### C. Stress relaxation

Three relaxation type experiments have been considered in order to further elucidate the nature of hard elasticity of precrazed

HIPS in qualitative terms. Although the relaxation processes are complex in nature, useful information can be gained from the way the system departs from the ideal case.<sup>2</sup> In a hard elastic system, relaxation processes are dominated by the more compliant fibrillar domains since they exist in a "matrix" which may be considered as an elastic solid.

#### 1. Effect of precrazing conditions

Figure 6 depicts the relative stress, i. e.,  $\sigma(t)/\sigma_0$ , as a semilogarithmic function of time for samples precrazed at 10, 40 and 70%, 10 minutes prior to the relaxation experiment. The level of precrazing did not affect the relaxation behavior substantially. When these results are compared with the relaxation results reported earlier for other hard elastic systems,<sup>2</sup> it becomes noticeable that the average rate of stress relaxation within the first two time decades matches that of PP and is much lower than that of poly(3-methylbutene-1) which is obvious from  $\sigma(2\text{min})/\sigma_0$  of each case.

As emphasized earlier,<sup>1, 3</sup> the stress relaxation of hard elastomers is resolvable into two components: a highly time dependent component prevailing in the short time region followed by a region in which the stress has very little or no time-dependency. It is the latter component ( $\sigma_\infty$ ) that has been considered to represent the "true" retractive force.<sup>1, 3</sup> The origin of each component and

how both can co-exist in the same system is discussed in a latter part of this report.

## 2. Effect of relaxation temperature

Figure 7 exhibits the stress relaxation behavior of precrazed HIPS at a fixed elongation of 40%. Here, the two regions discussed earlier were more obvious. During the short term region which prevails for the first decade, the rate of stress relaxation appeared to be temperature-independent. The temperature dependency became apparent in the long time region. It is to be noted that the material maintains its elastomeric nature at temperatures well above the highest relaxation temperature of this experiment (Fig. 4). The results shown here emphasize the thermoelastic results previously discussed (Fig. 5). In addition, the increased time dependency of the relaxation processes at higher temperatures accentuates the inherent viscoelastic nature of the system. Such viscoelastic effects have been concluded by Park and Noether<sup>15</sup> from more extensive stress relaxation investigations of hard elastic PP.

## 3. Effect of extension level

Figure 8 summarizes results of several stress relaxation experiments conducted at various extension levels. The data points represent an isochronous cross plot of the final load supported by the samples at 2 hours. Obviously, the final load (at 2 h) is proportional to the initial fixed elongation up to about 40% beyond which the load

supporting ability of the relaxed material starts to reach a constant level irrespective of the initial fixed elongation. A similar isochronous cross plot of the stress relaxation data of PP, reported recently by Cannon, Statton and Hearle,<sup>20</sup> reveals an identical behavior where "transition" to a constant final load starts at about 75% fixed elongation reaching a definite plateau at 100%. This behavior is explicable in reference to the first cycle stress-strain behavior of both HIPS and PP. For hard elastic HIPS (Fig. 1), the constant stress plateau (stage III) starts at about 40% elongation which corresponds to about 75% elongation in hard elastic PP (Fig. 9 of ref. 20). Since the stress relaxation of these systems is evidently a manifestation of the fibrillar component, it is therefore reasonable to suggest the following explanation. During deformation of the fibrillar-solid raw nucleated structure, a stage is reached where the fibrillar component approaches a state of very little or no deformation. Perhaps, it may be a state at which the orientation of the fibrillar material is maximum. The modulus of the composite approximates that of the solid component (be it lamellar in the crystalline material or amorphous bulk in the precrazed case) and the system behaves as a single component — an "elastic" solid displaying negligible stress relaxation.

Recently, an independent investigation on crystalline polymers has established that the controlling structural element in deformation

is the (interlamellar) non-crystalline regions.<sup>21</sup> More recently, Goritz and Muller<sup>11</sup> explained the lowered entropy of hard elastic PP observed during deformation by parallelization of the amorphous chains. Correlations of these results provide supportive evidence to the structural changes proposed.

D. Reaction to fluid environments

When a hard elastic material is extended to a fixed elongation, the stress relaxes to a time-independent level which has been considered as the "true" retractive force. The reaction of this stress level to liquid environments can be quite revealing to the nature of this force.

In this experiment, the film was first stretched in air to an initial elongation of 25% (the corresponding initial stress is about 54 kg/cm<sup>2</sup>), then relaxed for an hour after which it was immersed in the test liquid for 30 additional minutes. At that time, the liquid was removed and the film was allowed to "stress-relax" for 10 extra minutes. Figure 9 shows the stress relaxation behavior during the outlined course of the experiment. Whereas the stress showed no reaction to water, it was quite sensitive to formamide and Freon-E.<sup>3,22</sup> These three liquids are known to cause no swelling to PS, the liquid-polymer interaction would be dominated by surface effects. On one hand, the high surface tension of water did not cause it to wet PS fibrils and thus there was no effect on the stress level. Formamide

and Freon-E, on the other hand, due to their relatively low surface tension caused a spontaneous stress depression upon touching the sample (Arrow). Concurrent visual observations indicated that the depressed stress plateau was always reached when the liquid front had travelled across the width of the sample.

Upon removal of the liquid, the stress was suddenly elevated to a third time-independent level via a stress saddle whose origin is uncertain. The magnitude of the environmentally induced stress depression and elevation was noticed to depend on the fluid. Upon application of Freon-E fluid, for example, the stress dropped from  $53 \text{ kg/cm}^2$  (A) to another time independent level of  $39 \text{ kg/cm}^2$  (B) within 30 min, then rose sharply to  $46 \text{ kg/cm}^2$  (C) upon removal of the fluid. Whereas AB represents the total stress depression caused by the fluid, BC may represent its reversible component and AC the irreversible component. It is believed that the reversible component of the stress-depression is due to liquid-fibrillar surface interaction. The irreversible part, on the other hand, may encompass liquid entrapment due to the tortuous nature of the fibrillar structure, low evaporation rate, and/or permanent swelling effects. Although the total stress depression was found to be a strong function of the surface tension of the fluid, its reversible component was even stronger. Similar reversible stress displacement has been observed to occur in hard elastic polyethylene.<sup>3</sup>



Of course, the interaction between the strained hard elastic fibrillar structure and the environmental fluid is further complicated by other intricate factors such as the solubility parameter of the liquid and its viscosity. The complications involved may be demonstrated by the information listed in Table I, nevertheless, a correlation between the reversible stress depression by a liquid and its surface tension is easily deducible, taking into consideration possible viscosity and solubility parameter effects. Clearly, the spontaneous liquid-induced stress depression and elevation are strong indications that we are dealing with a high energy solid which must have resulted from the formation of fresh surface possibly during a fibrillation process. In order to minimize this surface energy, the total surface area tends to decrease since any surface contracts in order to decrease its surface energy. It has been shown<sup>23</sup> that this tendency creates considerable strain energy within the body (fibril). It is this internal energy which is believed to constitute the time-independent component of the stress, i. e., the "true" retractive force in the strained hard elastic material.

E. Strain-controlled fluid transport

When a hard elastic material is stretched, there is very little or no decrease in the cross-sectional area which must give rise to a substantial decrease in density. A marked increase in the inter-fibrillar voids have been characterized by conventional BET gas

adsorption and mercury porosimetry.<sup>7</sup> In this investigation, free sorption of high viscosity silicone oil, has been sought as another method in order to estimate the porosity of hard elastic HIPS. This method may also provide information about another potentially important property of the system, that is strain-controlled release.<sup>24</sup>

In one experiment, the sample, stretched to a fixed elongation, is allowed to stress-relax in air for 60 minutes after which high viscosity silicone oil (830 cP) is applied until the stress reaches the reduced time-independent level. Using a microbalance, the sample is then weighed to determine its oil uptake. In yet another experiment, the strain was released, continuously or intermittently, and the oil released was sorbed on preweighed filter paper clips and determined as a function of strain. Figure 10 summarizes results of such measurements carried out at 60% fixed elongation. A maximum oil uptake of about  $550 \text{ mg/cm}^3$  was found to be sorped by the strained film. From this value, a void fraction within the craze material under such conditions of about 0.47 is obtained. This value is in close agreement with values estimated from other more intricate techniques. This simple experiment provides a direct method for the evaluation of craze volume fraction directly under varying stress levels.

Of particular interest are the results of the controlled release of oil as a function of stress. While the sample was unloaded, the amounts of silicone oil released and retained by the sample was determined. As shown in the figure, the total amount released added to that retained would always match the total amount determined independently (solid triangle). The stress-controlled release process started very slow at high stress levels and was dramatically accelerated when the stress had reached 25% of its initial time-independent value. According to an over simplified view, it may be suggested that an actual compressive force was achieved at this level, thereby causing the accelerated release behavior. When the sample was totally unloaded, only a fraction of its maximum uptake had been released. More than half the oil sorbed by the sample remained entrapped within the tortuous structure of the craze material. Interestingly enough, even squeezing of the sample for excessive periods of time did not lead to the release of any substantial amount of oil. This behavior is obviously different from the established transport behavior of the same oil into PS crazes,<sup>25</sup> where the majority of oil was released within 24 hours under room conditions.

#### IV. MODELLING HARD ELASTIC BEHAVIOR

##### A. Structural observations

That hard elastic behavior had been thought of as a manifestation of raw crystallized polymers, the majority of the current models attributes the restoring force to some mechanism within the crystalline lamellae<sup>6-10</sup>. The discovery of hard elastic behavior of glassy polymers, in addition to the absence of lamellar shear or bending in the course of deformation of hard elastic crystalline polymers, requires a model that is in closer agreement with experimental observations.

The development of a model to explain hard elastic behavior has to be based upon information available. It is, therefore, appropriate to summarize the basic features established for hard elastic behavior.

1. The principal geometrical structure of hard elastic material, be it crystalline or glassy, is primarily composed of stacks of thin, flat, solid material bridged by extended fibrils. Both entities are uniaxially oriented in an alternate fashion with the applied stress.

2. The fibrils always exist in an extended form in the loaded and unloaded state.

3. Work recovery from a certain elongation appears to be constant and independent of the work of extension.

4. The thermoelastic coefficient is always negative.
5. The deformation stress of hard elastic material is composed of two components: time-dependent and time-independent.
6. Immersion in low surface energy liquids cause instantaneous reversible reduction of the time-independent stress.
7. No volume change accompanies elongation.

At the onset of this part of the discussion, it may be recalled that the stress-strain behavior recently famed as "hard elastic" clearly reminisces that of a single glassy polymer<sup>17, 18</sup> craze. Earlier, we have shown that the profuseness of this fibrillar unit (craze) in the system was essential for high elastic recovery from large extensions. Here, the basic unit is an extended fibrillar structure (elongated inclusion) in which the individual fibril is capable of undergoing reversible sequential subfibrillation in a hierarchial fashion. The evidence, based on the reported observation so far, suggests that a model describing this phenomenon should center about the extended fibril alternatively bridging solid entities. In what follows, we propose the sequential fibrillation model for hard elastic behavior.

Figure 11 idealizes the initial transformation of a native amorphous layer into craze or interlamellar fibrils. Whereas the "elastic" solid outside this layer may undergo very little or no deformation, the fibrillar material involved undergoes large extension possibly reaching several hundred percent.

Although the structural origin of the transformed layer in crystalline polymers is well established, it remains to be speculative in case of glassy polymers. Stress concentration caused by the rubber particles of HIPS enhances the development of such fibrillar structure (craze). A similar reasoning may be applied to "one phase" polymers, e. g., PC, where less densely packed regions have been postulated to enhance localized deformation.<sup>26</sup>

Due to the fact that the volume of the sample does not change during deformation and because of the lateral constraint imposed by the craze boundaries, Poisson's ratio effect causes the sequential subfibrillation of the involved chain molecules resulting in the creation of extremely large free surface. As illustrated in Fig. 12, if we consider an area of ca.  $1 \text{ mm}^2$  which is divisible into square lattice and that each square transforms into a single fibril, it may be possible to estimate the magnitude of free surface thus created. Such an estimate is facilitated by knowing the average fibrillar size. From microscopic observations, it is established that both inter-lamellar and craze fibrils are in the order of ca. 200 Å in diameter. A free surface in the order of  $10^5 \text{ mm}^2$  will be created during the fibrillation of  $1 \text{ mm}^2$ .

B. Estimation of possible values of retractive forces

If we consider a layer of specimen with initial cross sectional area  $A$  splitting into fibrils each having an average cross sectional

area of  $a$ , the number of fibrils  $n = A/a$ . For a given fiber with diameter  $d$ ,  $a = \pi d^2/4$  and  $n = 4A/\pi d^2$ . The free surface for a unit thickness thus created by the sequential fibrillation process may be estimated from the total perimeter of all newly created fibrils:  $S = n \pi d = 4A/d$ .

If the surface energy of the newly formed fibril,  $\gamma$ , is equal to that of the bulk polymer, the surface force per unit thickness can be evaluated as:  $F = \gamma S$ . An estimate of the surface forces thus induced in one square millimeter of polystyrene split into fibrils of varying diameters is shown in table 2. Here, the experimentally determined surface energy of bulk PS of 35 dynes/cm has been considered. On extending the specimen, there is a surface force accumulation that resists the extension. This idea stems from the fact that any surface contracts in order to decrease its surface energy.

Experimental observations have indicated that hard elasticity is resolvable into two components of different physical origin: an energetic component and a conformational one. Figure 13 schematically illustrates the possible coexistence of both types of elasticity within the same fibrillar unit. An elastic spring simulates the surface tension and a rubber-like rod models the conformational attribute of the macromolecular mass of the fibril. This model allows the fibril to be always in an extended form, loaded or unloaded. Of course, the characteristic relaxation time of the rod will determine its

specific time-dependent behavior. It is useful to recall that the time of relaxation is not only a material parameter, but is also size-dependent. At such a small fibrillar size, the time of relaxation is expected to be very small.

It is therefore obvious that the coexistence of these two properties within the fibril, given that fibrillation occurs in a sequential manner, can explain the hard elastic phenomenon without alluding to unrealistic assumptions.

C. Stress-strain behavior

A typical hard elastic cycle (extension and recovery) may be schematically represented as shown in Fig. 14. The initial elastic modulus reflects the composite nature of the system which is ideally composed of two phases: thin layers of solid material bridged by extended fibrils. The volume fraction of each component determine the magnitude of the initial elastic modulus. In general, the observed modulus value of precrazed HIPS is always less than that of the uncrazed material (Section III A).

At a critical stress, yield occurs signalling a complex process of sequential fibrillation and orientation. The stress state within the fibrillar domain may be visualized as shown in Fig. 15. Starting from the unloaded state (A) where we have an extended fibrillar bundles. Upon loading, each fibril is exposed to a triaxial stress state (B). Due to the effect of Poisson's ratio, further extension in the direction



of the applied stress causes contraction in the perpendicular direction which results in the splitting of the fibrils into subfibrils in a sequential manner. As the extension proceeds, the load-bearing fibrils will be so thin that a uniaxial stress state prevails. At this level, orientation becomes more dominant which is evidenced by the observed stress hardening and by the relatively high retractive modulus. It should be emphasized here, however, that the two major processes, sequential fibrillation and orientation, may occur simultaneously.

Another critical stage of deformation may be reached in some cases, depending on the processing conditions, in which a constant stress deformation occurs (stage III). The stress plateau is believed to signal the pulling of additional fibrillar material from the "solid" boundaries.

An important feature of the model is the reversibility of the sequential fibrillation process upon load reversal. This can be easily understood in light of the fact that attraction due to secondary forces (e. g. , van der Waals) is sufficient to produce adhesive joints between polymers of strength equal to that of the polymers themselves without the need for chemical bonds. The freshly formed sub and microfibrils remain within very close distance that reformation of fibrils is practically feasible.

## V. CONCLUSIONS

When profusely precrazed under uniaxial tension, high impact polystyrene is converted into hard elastic material. Examination of the stress-strain behavior under various loading conditions reveals that precrazed HIPS exhibits characters typically displayed by highly crystalline hard elastic materials. Response of the retractive force to liquid environmental changes has been scrutinized in order to determine the physical mechanism governing hard elasticity. The major conclusions of this study are summarized below:

1. Hard elastic HIPS shows abnormally high recovery from large extensions at which no changes in the cross-sectional area are observed. High elastic recovery persists at temperatures close to the glass transition.
2. Precrazing intensity, time elapsed after precrazing (shelf life) and test temperature exert a marked effect on the extension path. However, the retractive path and the work recovery from a certain elongation are always independent of the extension history.
3. Continuous repeated cycling of precrazed HIPS leads to a stable extension and retraction curve with relatively high elastic and work recovery. Intermittent repeated cycling, on the other hand, affect healing of the structure towards bulk properties.

4. A negative slope in the retractive stress-temperature relationship is shown, concluding that the elasticity is not rubber-like but controlled by internal energy effects.

5. Low surface liquids cause reversible depression of the retractive force which indicates that surface forces dominate the elastic recovery.

6. A new method for the measurement of internal porosity under stress is introduced. The method is based on stress-induced sorption and release of high viscosity fluids. Preliminary measurements show that hard elastic HIPS possesses remarkable porosity which can be utilized for the storage and controlled release of viscous fluids.

7. A new structural model is proposed to explain the observed mechanical and structural data. Based on strain-induced sequential subfibrillation, the model predicts an extensive, yet reversible, creation of new surface area as a result of straining the original composite structure. The free surface energy associated with the new subfibrillar surface provides the retractive force observed.

### ACKNOWLEDGEMENTS

The authors gratefully acknowledge the generous support of this project through the Office of Naval Research—Contract Number N00014-75-C-0795 and the National Science Foundation—Grant Number DMR 77-24952. We are most thankful to Dr. B.S. Sprague of Celanese for his helpful comments and to Drs. Anderson and England of Dupont Co. for supplying Freon fluids. The contribution of Mr. M. Rackovan of CIT is also appreciated.

## REFERENCES

1. M. J. Miles and E. Baer, J. Mater. Sci., 14, 1254 (1979).
2. S. L. Cannon, G. B. McKenna and W. O. Statton, Macromol. Rev., 11, 209 (1976).
3. M. J. Miles, J. Petermann and H. Gleiter, J. Macromol. Sci.-Phys., B12(4), 523 (1976).
4. H. D. Noether, Intern. J. Polymeric Mater., 7, 57 (1979).
5. M. E. Mackay, T. G. Teng and J. M. Schultz, J. Mater. Sci., 14, 221 (1979).
6. E. S. Clark, "Structure and Properties of Polymer Films", edited by R. W. Lenz and R. S. Stein (Plenum, New York, 1973).
7. B. S. Sprague, J. Macromol. Sci.-Phys., 8, 157 (1973).
8. R. P. Wool, J. Polym. Sci.-Phys., 14, 603 (1976).
9. H. Cackovic, J. L. Cackovic, R. Hosemann and D. Goritz, J. Macromol. Sci.-Phys., 16, 145 (1979).
10. H. Ishikawa, H. Numa and M. Nagura, Polymer, 20, 516 (1979).
11. D. Göritz und F. H. Müller, Colloid Polym. Sci., 253, 844 (1975).
12. T. Hashimoto, A. Todo, Y. Tsukahara and H. Kawai, Polymer, 20, 636 (1979).
13. A. Y. Coran and R. Patel, J. Appl. Polym. Sci., 20, 3005 (1976).
14. R. G. Quyn and H. Brody, J. Macromol. Sci.-Phys., B5(4), 721, (1971).
15. I. K. Park and H. D. Noether, Colloid Polym. Sci., 253, 824 (1975).
16. K. Takahashi, J. Polym. Sci.-Phys., Ed., 12, 1697 (1974).

17. R. P. Kambour and R. W. Kopp, J. Polym. Sci., A2(7), 183 (1969).
18. J. Hoare and D. Hull, Phil. Mag., 26, 443 (1972).
19. C. B. Bucknall, Brit. Plast., 40(12), 84 (1967).
20. S. L. Cannon, W. O. Statton and J. W. S. Hearle, Polym. Eng. Sci., 15(9), 633 (1975).
21. R. J. Samuels, J. Macromol. Sci. -Phys., B8(1-2), 41 (1973).
22. Freon-E 3 Series Fluorocarbons, E. I. DuPont DeNemours & Co.
23. K. Jagannadam and M. J. Marcinkowski, J. Mater. Sci., 14, 1717 (1979).
24. A. Moet and E. Baer, Proceedings of VI Inter-American Conf. on Materials Technology, San Francisco (1980).
25. A. Moet and E. Baer, J. Mater. Sci., 15, 31 (1980).
26. S. Wellinghoff and E. Baer, J. Appl. Polym. Sci., 22, 2025 (1978).

### TABLE CAPTIONS

TABLE I. Depression of retractive stress caused by immersion in liquid environments as a function of their surface tension, solubility and viscosity.

TABLE II. As estimation of surface forces associated with the new surface created by subfibrillation of a low dimensional layer of  $1 \text{ mm}^2$ .

### FIGURE CAPTIONS

- Fig. 1 Typical stress-strain curves for hard elastic HIPS precrazed at 30, 50 and 70%.
- Fig. 2 Effects of cycling loading on the hard elastic behavior of HIPS precrazed to 40% elongation, [a] 12 continuous cycles (arrow indicating first cycle), and [b] three intermittent cycles.
- Fig. 3 Effects of time elapsed between precrazing and testing on the "hard" elastic behavior of HIPS.
- Fig. 4 Effects of test temperature on the hard elastic behavior of samples precrazed at room temperature.
- Fig. 5 Thermoelastic behavior of hard elastic HIPS at 25% fixed elongation.
- Fig. 6 Stress relaxation behavior as affected by precrazing elongation.
- Fig. 7 Effect of temperature on the stress relaxation behavior of precrazed HIPS
- Fig. 8 Effect of the fixed extension level on the final load after 2 hours of stress relaxation. All samples were precrazed to 40%.
- Fig. 9 Stress relaxation behavior of hard elastic HIPS in air for one hour then in liquid (arrow) for 30 minutes.
- Fig. 10 Sorption and release of high viscosity silicone oil (500 cS) as function of stress.



- Fig. 11            Schematic illustration of the layer transformed into crazed material depicting the stress state exerted on a fibrillar unit.
- Fig. 12            Sequential fibrillation envisioned in an area of  $1\text{mm}^2$  across the layer shown in Fig. 10.
- Fig. 13            Schematic illustration of possible coexistence of surface forces (spring) together with conformational property of the fibrillar mass so that the fibril is always in an extended state; loaded or unloaded.
- Fig. 14            Extension and retraction behavior of hard elastic material in association with reversible subfibrillation.

TABLE I

Liquid	Viscosity (cP)	Surface Tension (dynes/cm)	Solubility Parameter (cal/cm <sup>3</sup> )	Depression of refractive stress Total (kg/cm <sup>2</sup> )	Reversible (kg/cm <sup>2</sup> )
Water	1.0	72.0	23.61	0	
Formamid	3.3	58.2	19.2	4.5	4.0
Acetic Acid	1.2	28.8	10.1	45.7	13.2
Methanol	0.6	24.5	14.5	25.9	16.6
Ethanol	1.0	24.0	10.0	31.3	24.7
Silicone Oil <sup>2</sup>	8300	21.3		13.5	
"	830	21.1	4.9 to 5.9	19.8	
"	8.3	19.7		21.4	
"	1.7	19.2		30.5	13.7
n-Hexane	0.3	18.4	7.3	53.9	23.7
Freon (E-3) <sup>1</sup>	2.2	14.2	5.2 <sup>3</sup>	13.5	7.8

1. Fluorocarbon liquid (Du Pont Co.)

2. Polydimethylsiloxane

3. Estimated

TABLE II

Fibrillar diameter (A)	500	250	100
Total Perimeter, S, (mm)	$0.8 \times 10^5$	$1.6 \times 10^5$	$4 \times 10^5$
Force (Kg)	0.28	0.56	1.40

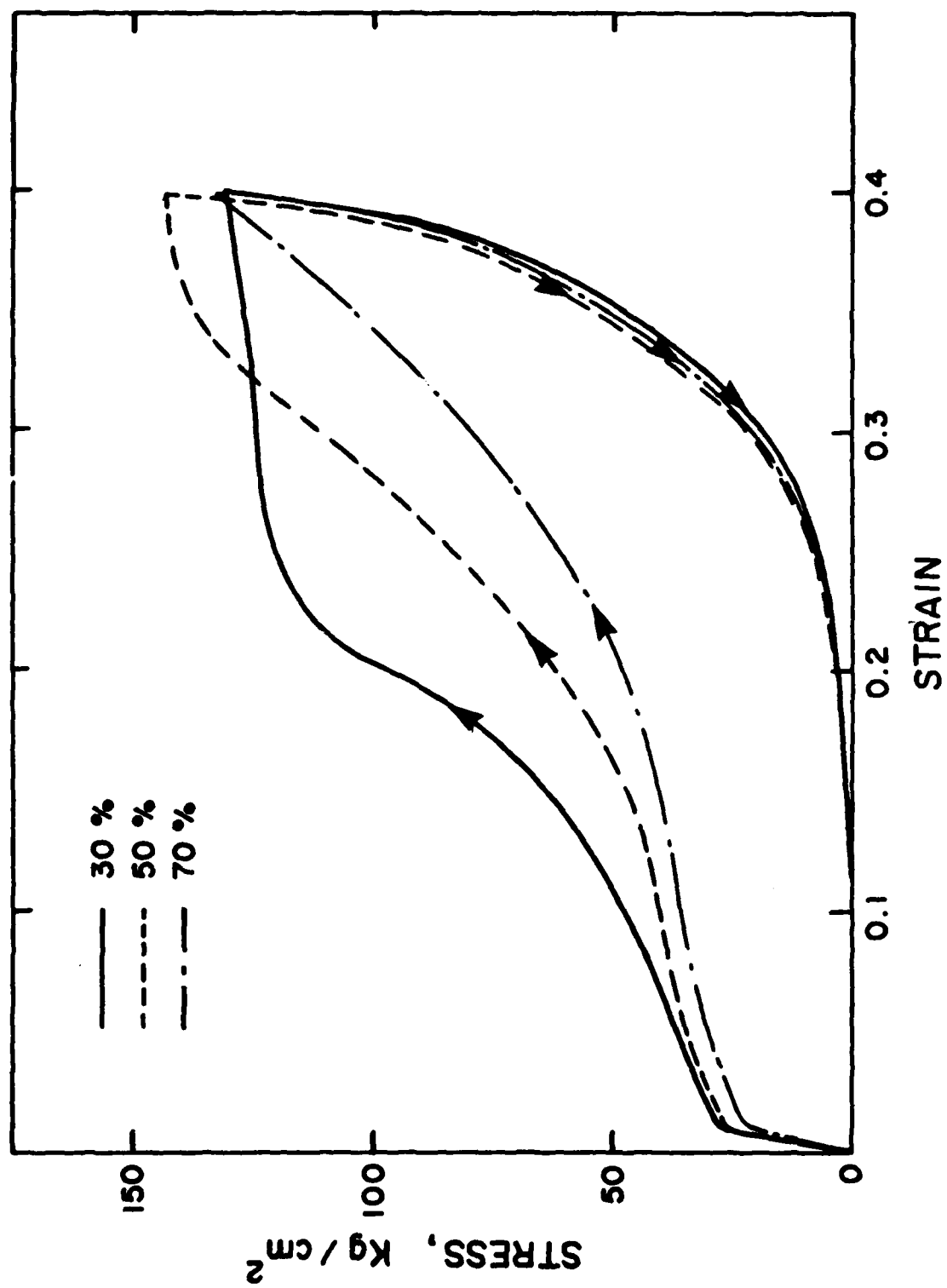


Fig. 1

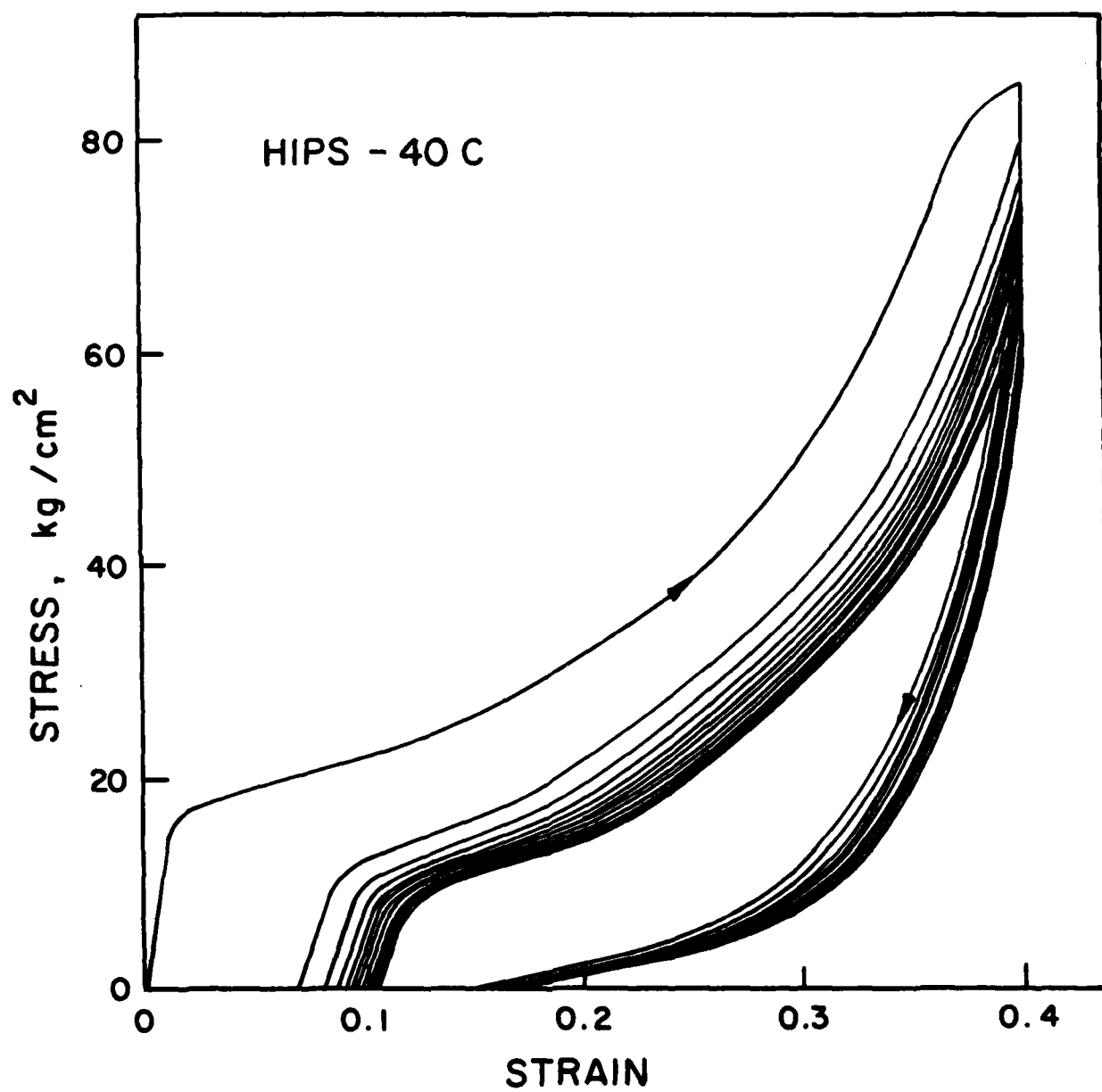


Fig. 2a

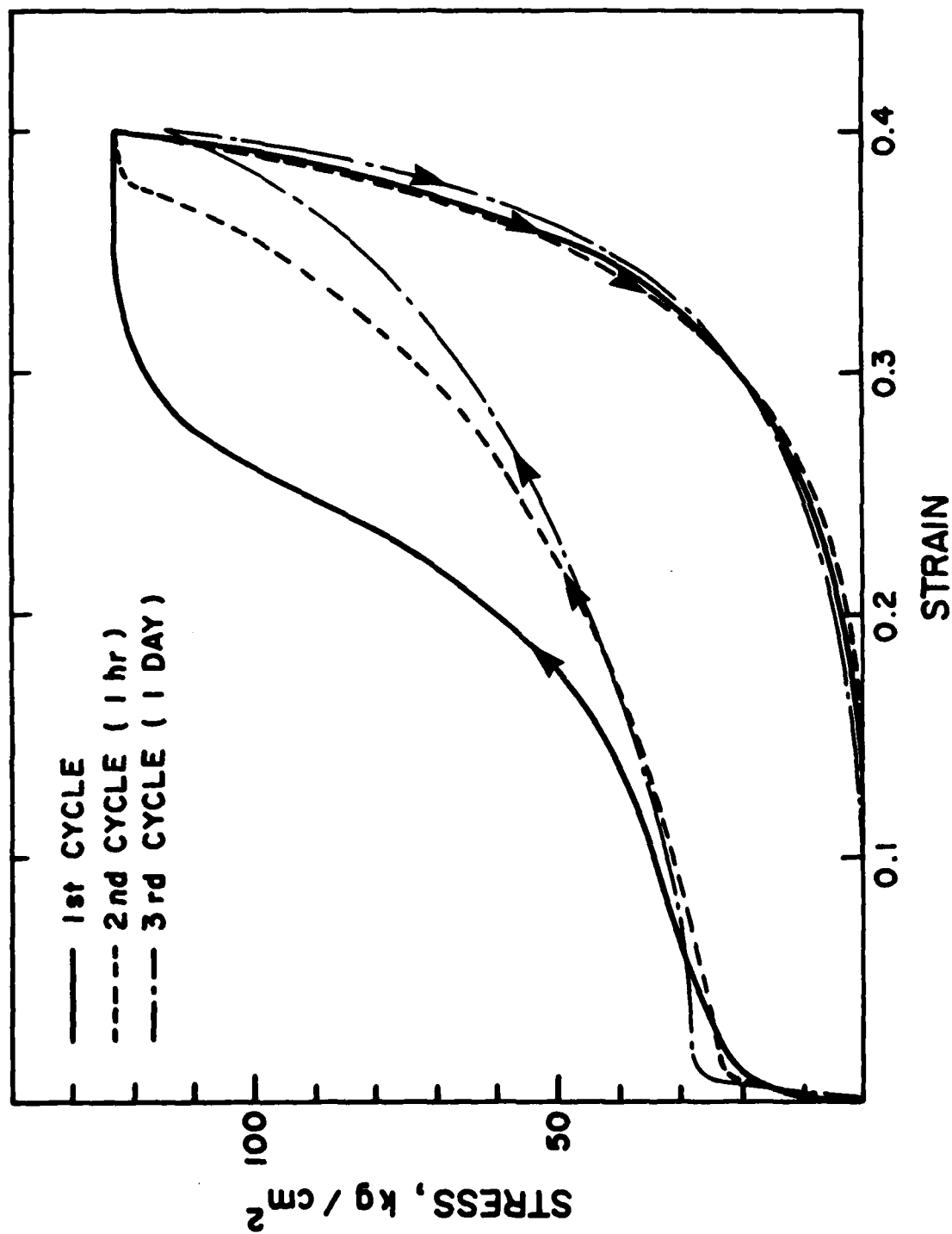


Fig. 2b

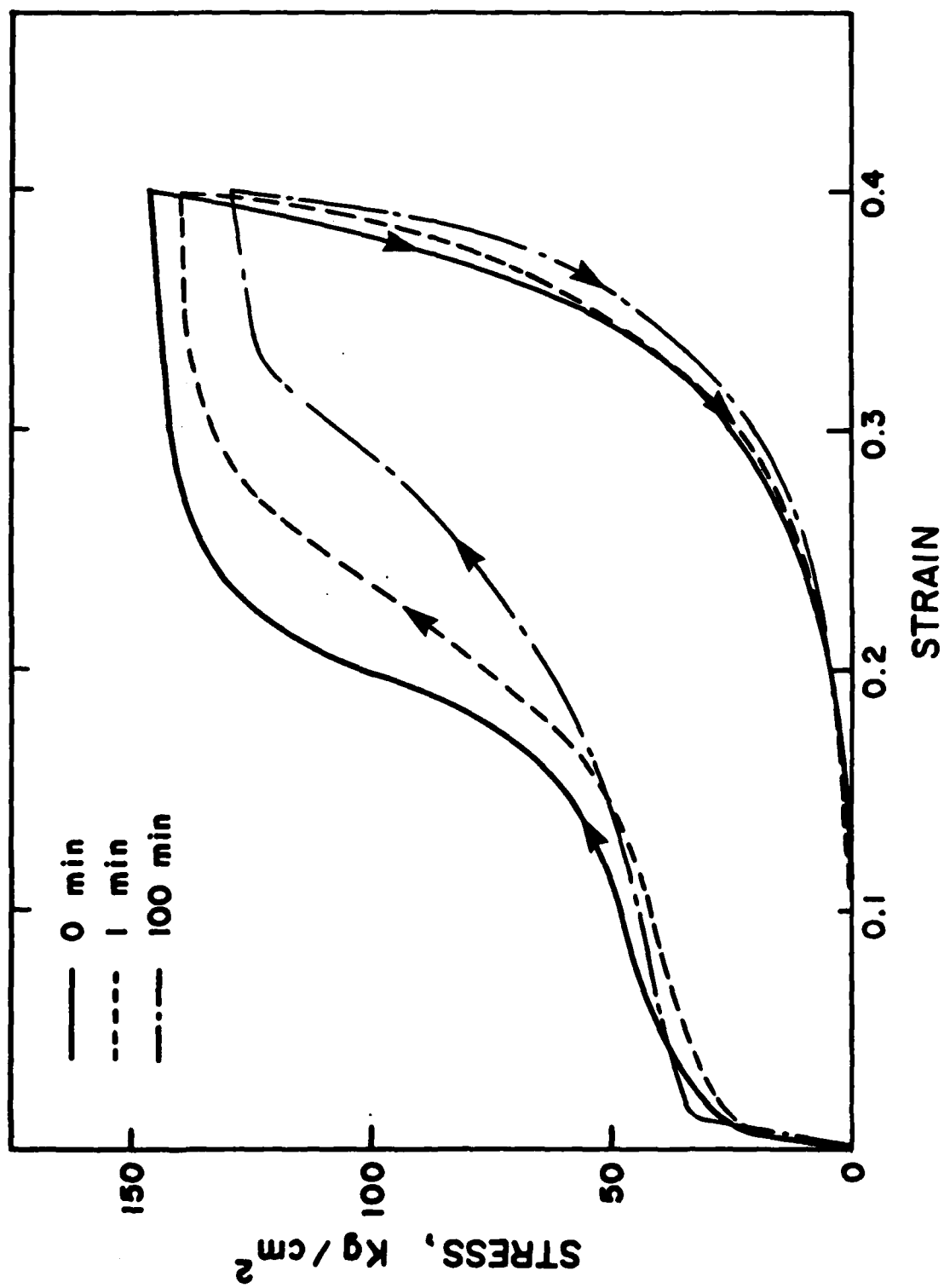


Fig. 3

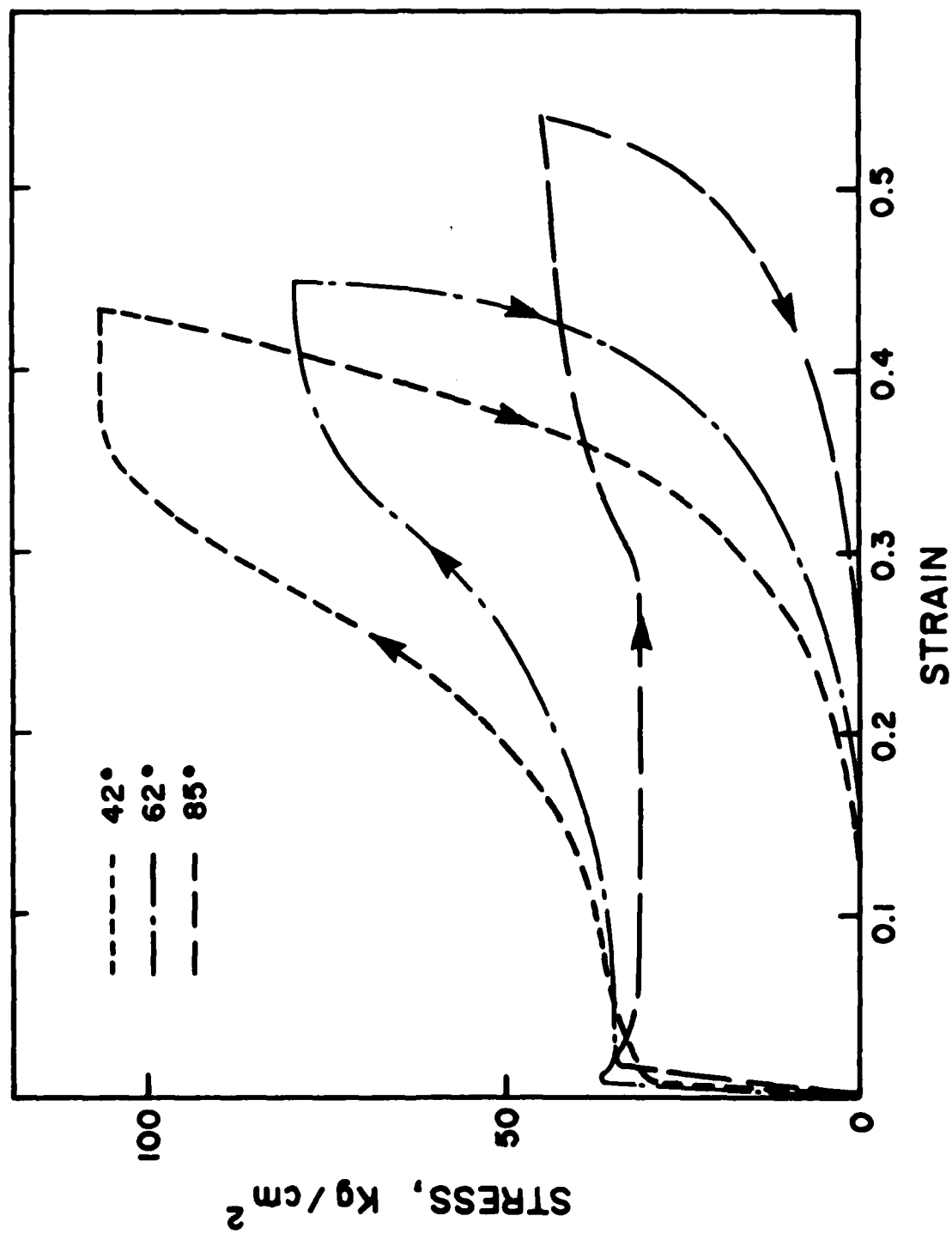


Fig. 4



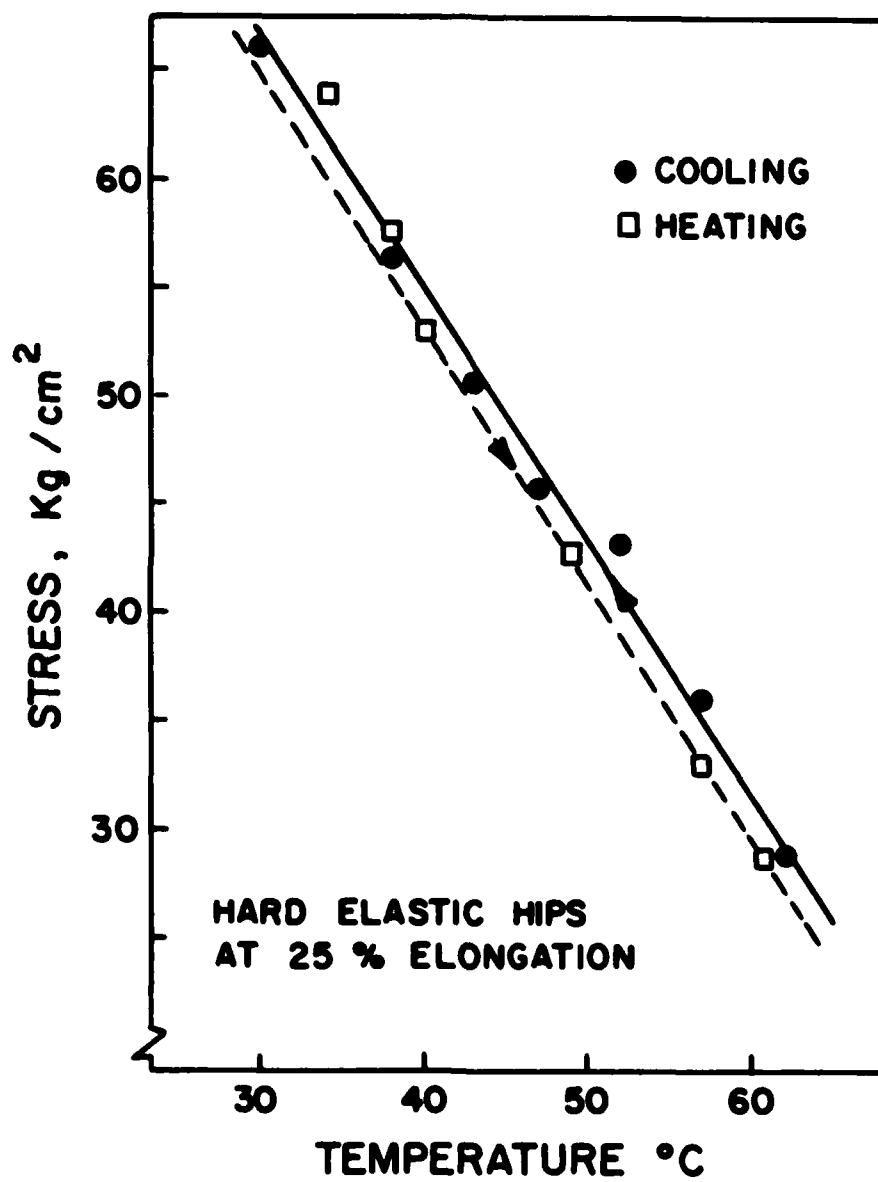


Fig. 5

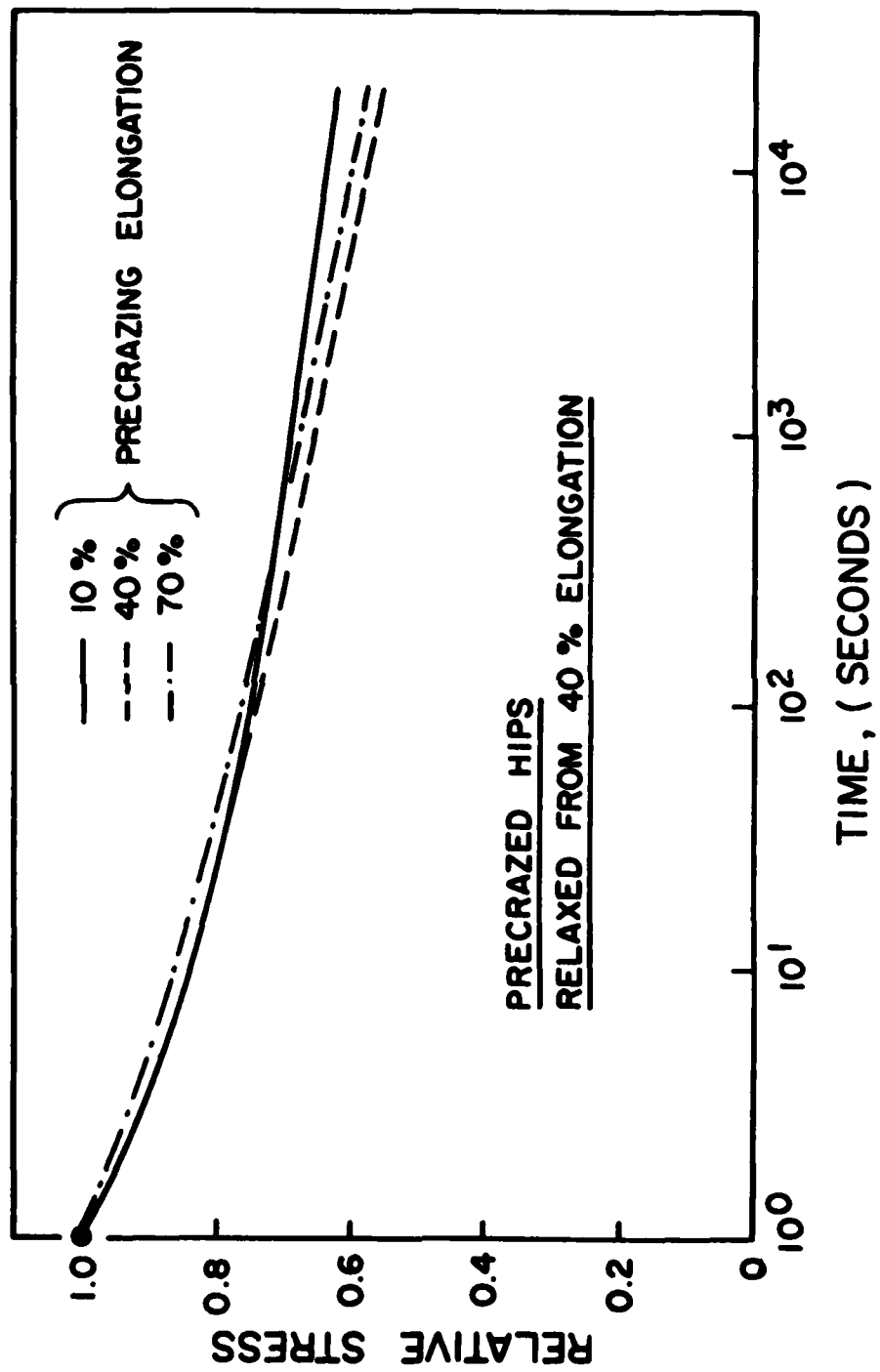


Fig. 6

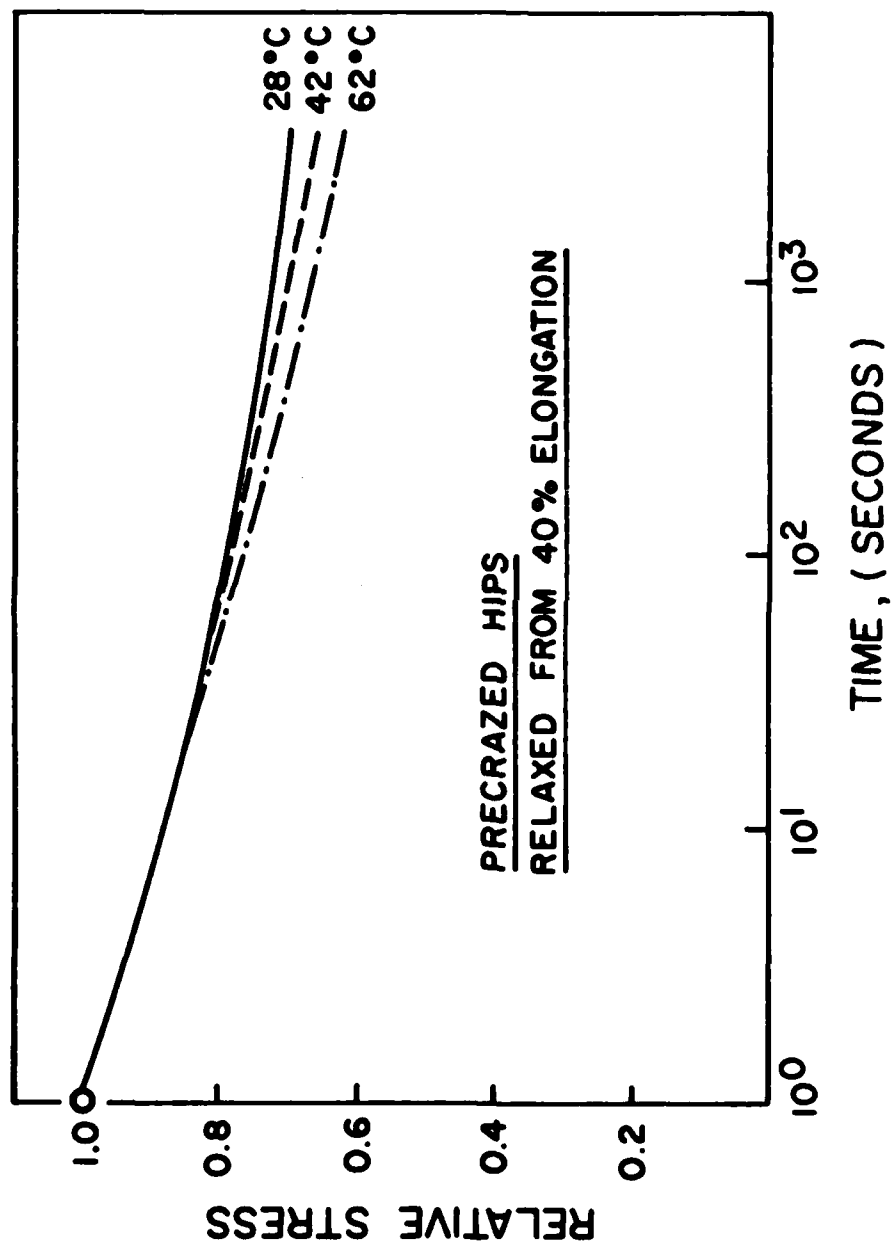


Fig. 7

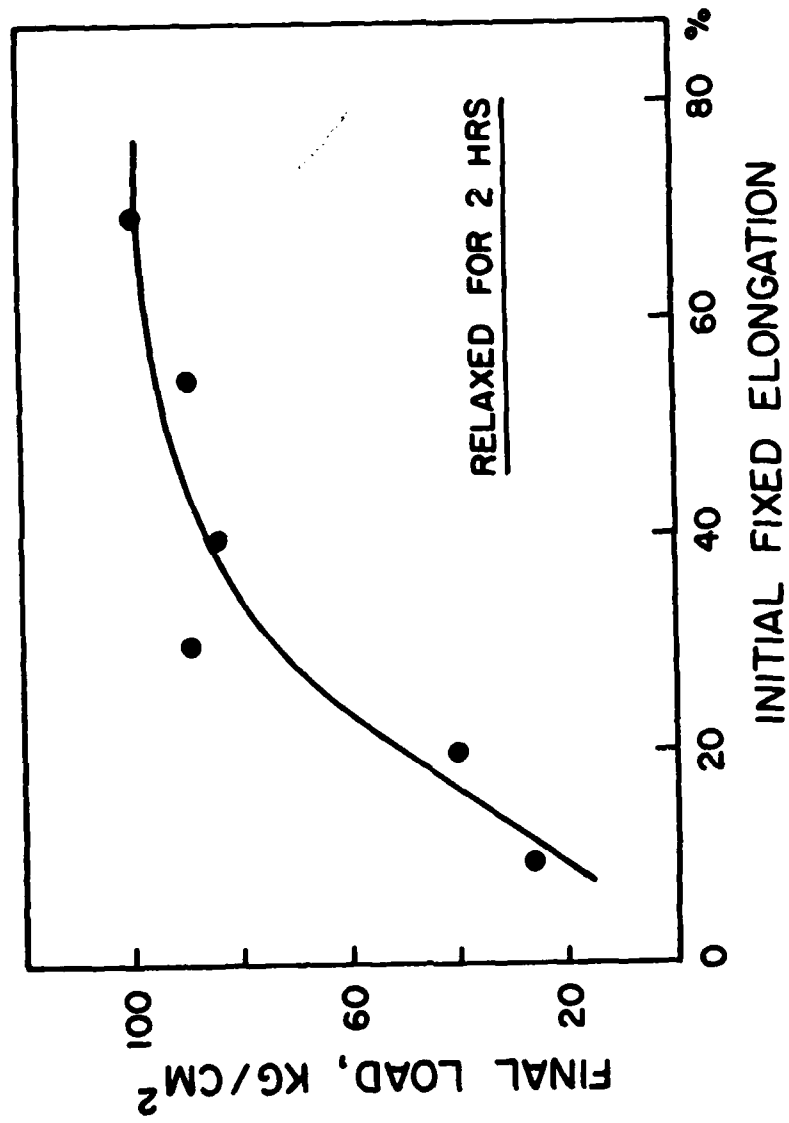


Fig. 8

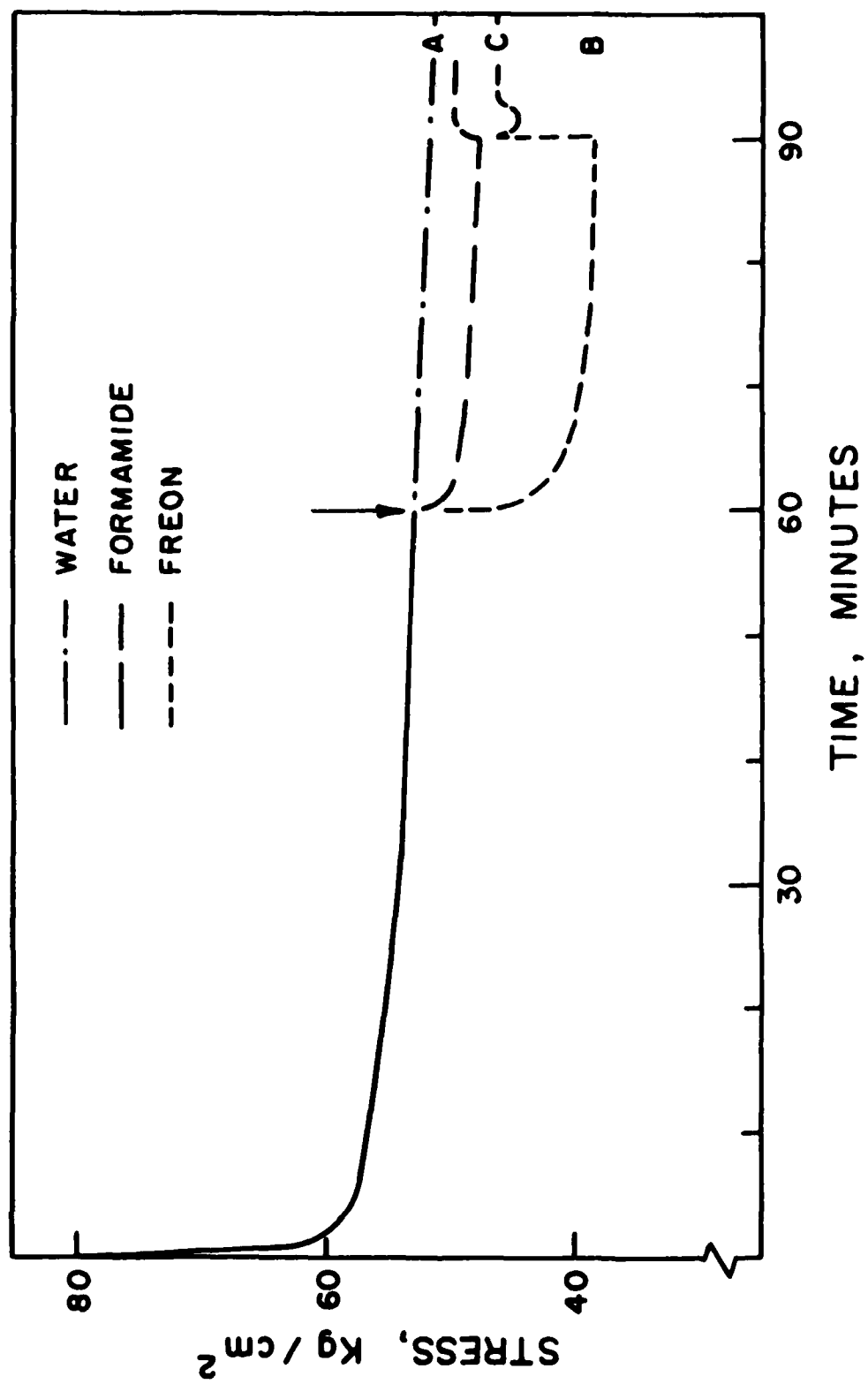


Fig. 9

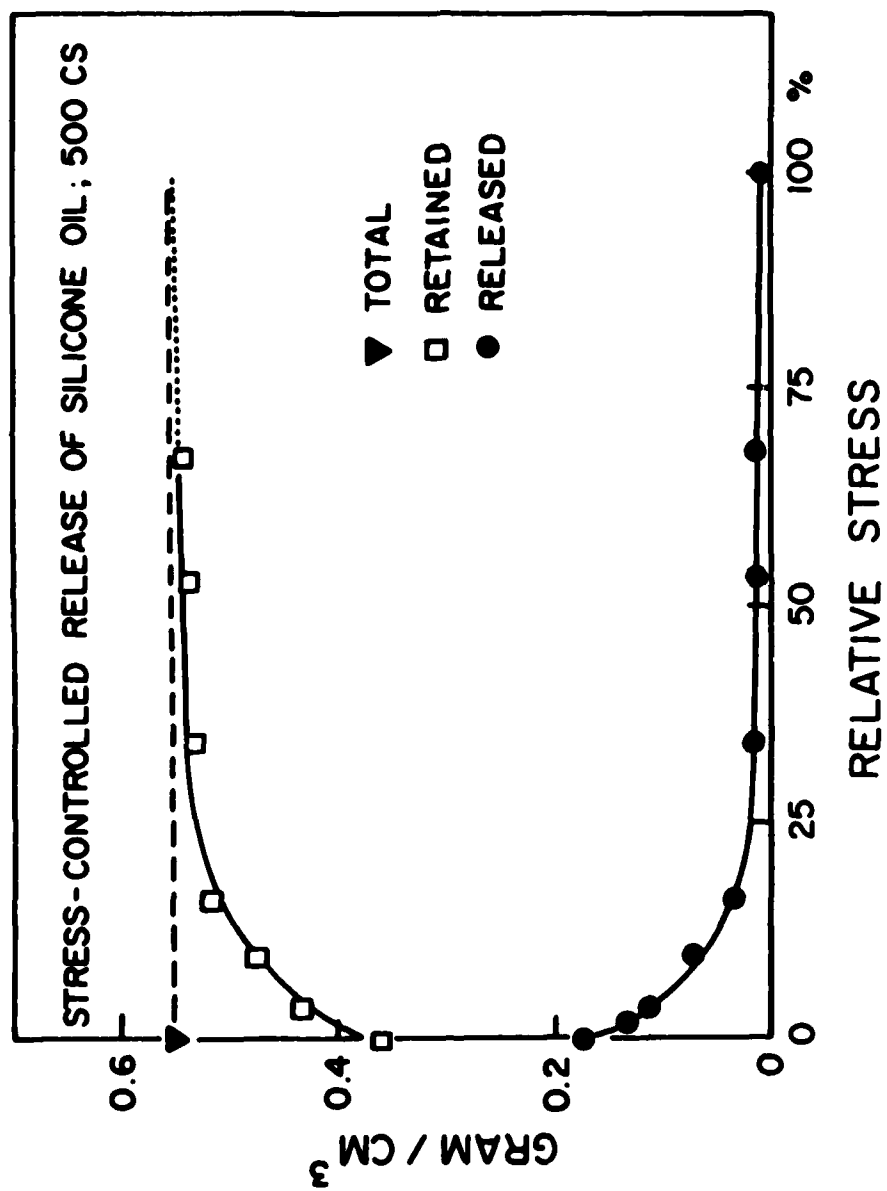


Fig. 10

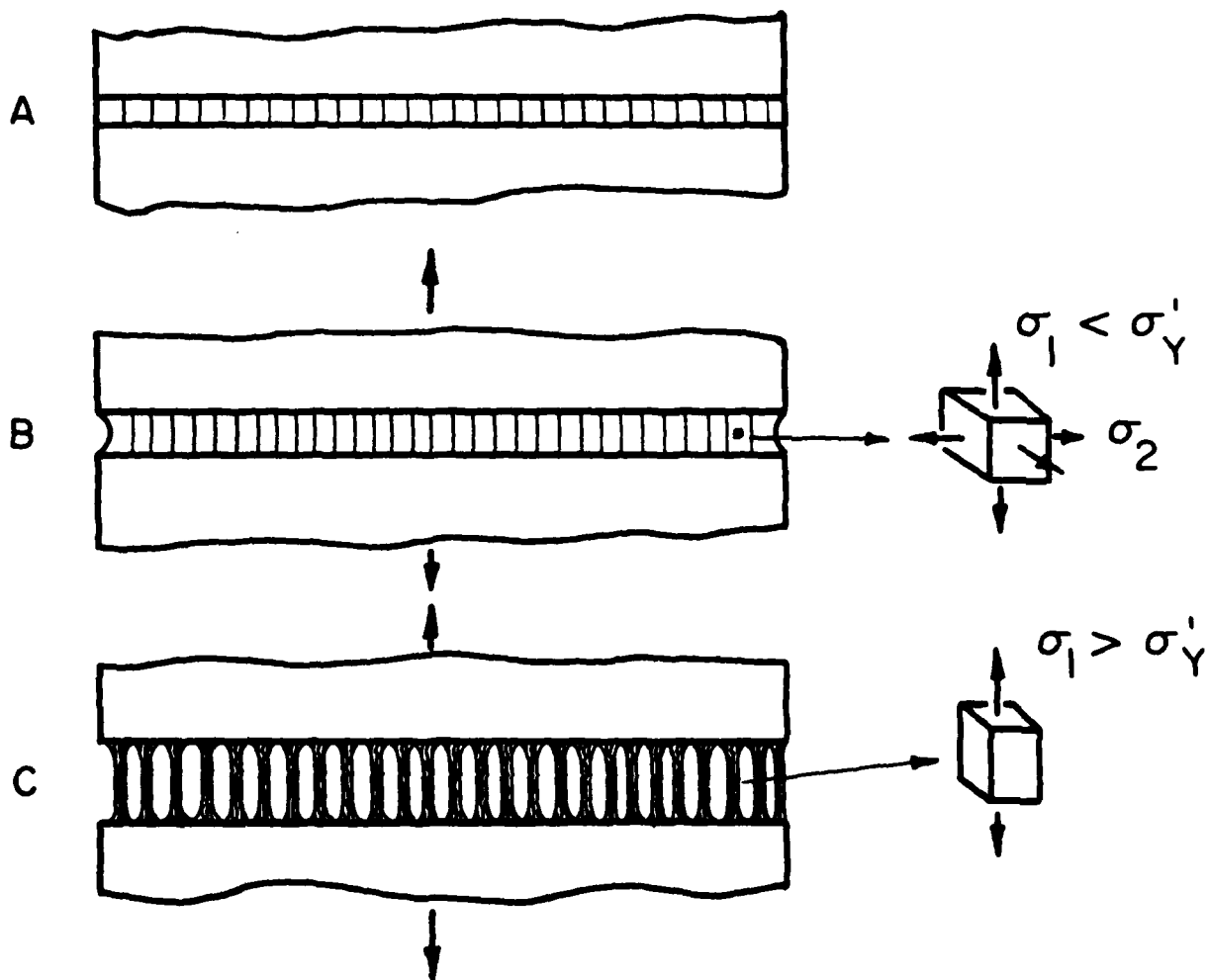


Fig. 11

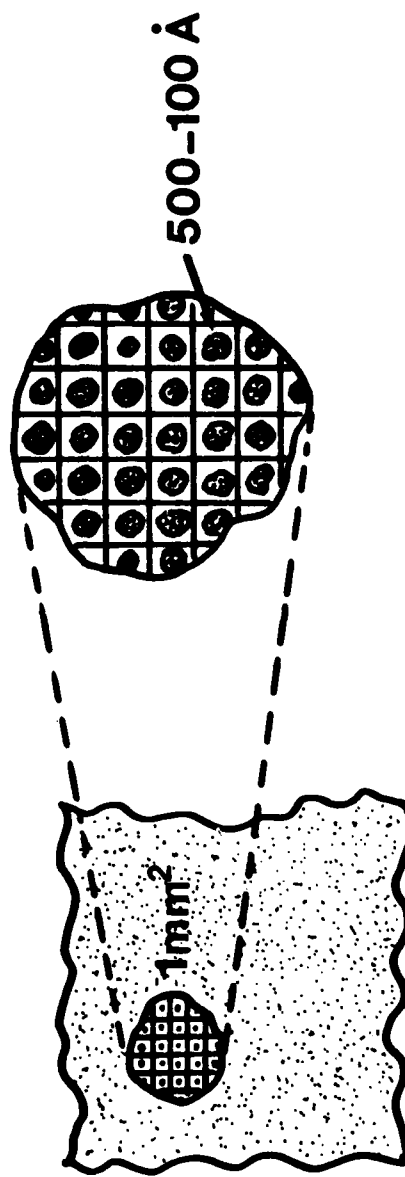


Fig. 12



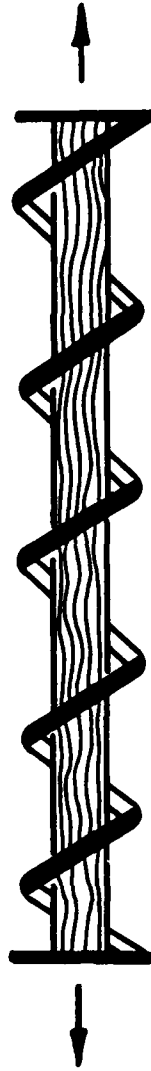
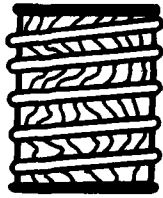


Fig. 13

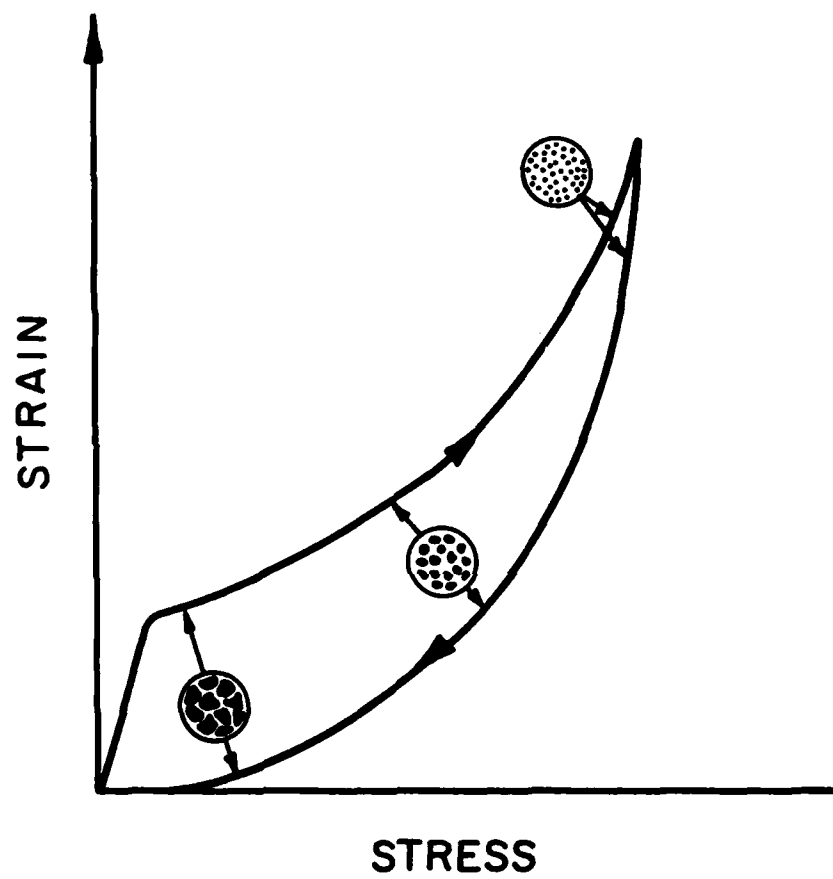


Fig. 14

DATA  
FILM

